

of $0.0 \pm 4\%$ deuterium incorporation. There was 6% of the styrene present in the solvolysis product as indicated by the VPC trace, but based on the known reactivities of substituted styrenes in TFA²⁶ this material is expected to be inert under these conditions.

The reaction of **8c** in CD₃CO₂D was similarly observed by ¹H NMR and no deuterium incorporation in the CHCH₃ of the product was detectable.

Acknowledgment. Financial support of this research was provided by the Natural Sciences and Engineering Research Council

of Canada. We thank Dr. M. Charpentier (CNRS, Thiais, France) for helpful discussion made possible by a NATO collaborative research grant, Professor X. Creary for providing unpublished results (ref 21e), and Professor A. R. Stein for the resolution procedure (ref 16).

Supplementary Material Available: Tables of ¹H NMR spectra, elemental analysis, and mass spectral data (4 pages). Ordering information is given on any current masthead page.

Electronic Structure and Bonding of the Blue Copper Site in Plastocyanin

Kevin W. Penfield, Andrew A. Gewirth, and Edward I. Solomon*

Contribution from the Department of Chemistry, Stanford University, Stanford, California 94305. Received October 10, 1984

Abstract: Spin restricted self consistent field-X α -scattered wave (SCF-X α -SW) calculations are presented for a number of approximations to the blue copper active site in plastocyanin. The results of these calculations indicate that the bonding at the site is quite covalent and that substantial electron delocalization occurs. A comparison of X α calculations for free imidazole and the blue copper site indicates that the splitting of the imidazole π_1 and π_2 and n and π_2 levels is expected to significantly increase upon complexation. Similarly, the 2e and 3a₁ valence levels of the methylthiolate ligand split into three levels upon complexation to copper. The energy separation between these levels is calculated to decrease relative to the splitting between the 2e and 3a₁ levels in free methylthiolate. All three valence levels have significant electron delocalization onto the copper, and the bonding is best described as involving one π - and two σ -type interactions. The 4a₁ (sulfur p_z) orbital of the axial thioether ligand at the blue copper site is computed to undergo a small but significant bonding interaction with the d_{z²} orbital on the copper. On the basis of comparison to D_{4h} CuCl₄²⁻ and CuCl₆⁴⁻ model complexes, this interaction is found to effect the energy of the d_{z²} \rightarrow d_{x^{2-y²}} ligand field transition. Formalisms are developed to calculate g and A values from the output of the X α calculation. The g values provide an experimental calibration for the amount of delocalization present in the ground state wave function. These calculations indicate that the unpaired electron in the blue copper site spends about 40% of the time in a d_{x^{2-y²}} orbital on the copper and about 36% of the time on the p π orbital of the thiolate sulfur. A rhombic splitting of 0.017 in the g values is calculated, the magnitude of which is confirmed by experimental observation of this splitting in spinach plastocyanin with Q-band EPR. The rhombic character of the EPR appears to relate to electron delocalization of the ground state wave function over the p π orbitals of the sulfur. Hyperfine values are calculated for the blue site and for D_{4h} CuCl₄²⁻. The difference between the values for the two complexes is found to relate in large measure to the increased delocalization in the blue site relative to CuCl₄²⁻. p_z mixing at the blue site is not found and is shown to be insufficient as an explanation for the reduced A_z in the blue site relative to D_{4h} CuCl₄²⁻. These studies provide a reasonable, experimentally calibrated, approximation of the orientation and delocalization of the ground state wave function involved in electron transfer.

I. Introduction

The blue copper active site is found in a number of proteins containing single copper centers, including the plastocyanins, azurins, and stellacyanins.¹ This site is also found in the multicopper oxidases: laccase, ceruloplasmin, and ascorbic acid oxidase. In those proteins where the function of the blue copper site has been clearly determined, it participates in outer-sphere electron-transfer reactions. There has been a great deal of effort focused toward understanding the spectral features and associated electronic structure and bonding of the blue copper site, with the long-range goal of relating the unusual electronic structure properties to active-site reactivity.

Spectroscopy on the blue copper active site has focused on understanding the unique spectral features of the site in terms of its geometry.² These spectral features include an unusually small copper hyperfine splitting of the EPR signal in the g_{\parallel} region ($A_{\parallel} \leq 70 \times 10^{-4} \text{ cm}^{-1}$) and an extremely intense low-energy absorption band ($\nu \approx 600 \text{ nm}$, $\epsilon \approx 4000 \text{ m}^{-1} \text{ cm}^{-1}$). Infrared

circular dichroism (IRCD) studies³ demonstrated that at least three d-d transitions existed in the blue copper proteins at wavelengths as large as 2 μm . A ligand-field analysis³ of these transitions indicated that the site has a geometry close to tetrahedral and that all d-d transitions would have to occur at energies below 800 nm. Therefore, the intense 600 nm absorption band must involve a charge-transfer (CT) transition, which probably arises from cysteine ligation⁴ at the site. High-resolution structures of plastocyanin⁵ (to 1.6 Å) and azurin⁶ (to 2.7 Å) indicate that the remaining ligands are two imidazoles of histidine and a

(1) (a) Malkin, R.; Malmstrom, B. G. *Adv. Enzymol.* **1970**, *33*, 177-244. (b) Fee, J. A. *Struct. Bonding (Berlin)* **1975**, *23*, 1-60.

(2) (a) Gray, H. B.; Solomon, E. I. In "Copper Proteins"; Spiro, T. G., Ed.; Wiley: New York, pp 1-39. (b) Solomon, E. I.; Penfield, K. W.; Wilcox, D. E. *Struct. Bonding (Berlin)* **1983**, *53*, 1-57. (c) Solomon, E. I. In "Copper Coordination Chemistry: Biochemical & Inorganic Perspectives"; Karlin, K., Zubieta, J., Eds.; Adenine Press: Guilderland, N.Y., 1982, pp 1-22.

(3) (a) Solomon, E. I.; Hare, J. W.; Gray, H. B. *Proc. Natl. Acad. Sci. U.S.A.* **1976**, *73*, 1389-1393. (b) Solomon, E. I.; Hare, J. W.; Dooley, D. M.; Dawson, J. H.; Stephens, P. J.; Gray, H. B. *J. Am. Chem. Soc.* **1980**, *102*, 168-178.

(4) (a) Katoh, S.; Takamiyama, A. *J. Biochem. (Tokyo)* **1964**, *55*, 378. (b) Solomon, E. I.; Clendening, P. J.; Gray, H. B.; Grunthaner, F. J. *J. Am. Chem. Soc.* **1975**, *97*, 3878. (c) Wurzbach, J. A.; Grunthaner, P. J.; Dooley, D. M.; Gray, H. B.; Grunthaner, F. J.; Gay, R. R.; Solomon, E. I. *J. Am. Chem. Soc.* **1977**, *99*, 1257. (d) Thompson, M.; Whelan, J.; Zemon, D. J.; Bosnich, B.; Solomon, E. I.; Gray, H. B. *J. Am. Chem. Soc.* **1979**, *101*, 2482. (e) Solomon, E. I.; Rawlings, J.; McMillin, D. R.; Stephens, P. J.; Gray, H. B. *J. Am. Chem. Soc.* **1976**, *98*, 8046. (f) McMillin, D. R.; Holwerda, R. A.; Gray, H. B. *Proc. Natl. Acad. Sci. U.S.A.* **1974**, *71*, 1338. (g) McMillin, D. R.; Rosenberg, R. C.; Gray, H. B. *Proc. Natl. Acad. Sci. U.S.A.* **1974**, *71*, 4428.

(5) Guss, J. M.; Freeman, H. C. *J. Mol. Biol.* **1983**, *169*, 521-63.

(6) Adman, E. T.; Jensen, J. H. *Isr. J. Chem.* **1981**, *21*, 8.

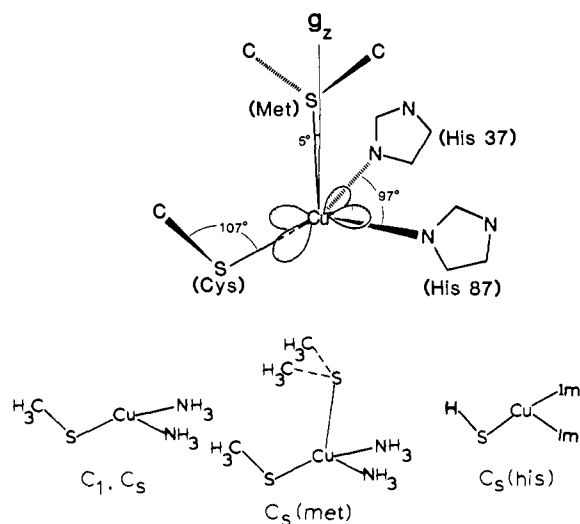


Figure 1. Top: electronic structural representation of the plastocyanin active site. The direction of g_z was determined experimentally, while the orientation of the $d_{x^2-y^2}$ orbital was estimated from ligand-field calculations. Note that the bonds from Cu to N(his 37), N(his 87), and S(cys) are all less than 15° below the xy plane. From ref 7. Bottom: the four approximations to the blue copper site considered in this paper.

thioether from methionine. While the length of the imidazole to copper bond is fairly normal when compared to model complexes, the Cu-S (thiolate) bond is found to be quite short (2.1 Å) and the Cu-S (thioether) bond is quite long (2.9 Å).

Subsequent polarized optical studies⁷ in combination with variable-temperature absorption, CD, and MCD spectroscopies³ showed that at least five transitions are present in the CT region of plastocyanin. The polarized single-crystal studies indicated that Cu-S thioether transitions contribute at most weakly to the absorption spectrum, a feature which raises a significant question concerning the nature of the copper-thioether bond. The absence of a bond between the copper and the thioether at the blue copper site has, in fact, been considered as a possibility based on resonance Raman⁸ and EXAFS⁹ studies.

A correlation of the five optical transitions with the polarized single-crystal absorption spectra⁷ indicated that three thiolate to Cu CT transitions may be present. In plastocyanin, the cysteine C-S-Cu angle is significantly less than 180° . This bent bond should split the doubly degenerate π set of orbitals. Thus, the strong interaction of the sulfur with the carbon of the cysteine residue results in three rather than two transitions.

Single-crystal EPR⁷ spectra of plastocyanin in conjunction with a ligand-field calculation demonstrated that the g^2 and A^2 tensors are colinear and the g_z is 5° off the Cu-S (methionine) axis. Thus, the $d_{x^2-y^2}$ orbital, which is perpendicular to g_z and contains the unpaired electron, is less than 15° above the plane formed by the S (cysteine) and the two N (histidine) ligands. This orientation of the $d_{x^2-y^2}$ orbital is reproduced in Figure 1. The ligand-field calculations further indicated that if the rhombic splitting is removed, only the C_{3v} energy level ordering is found to be reasonable, the long axis being along the Cu-thioether bond, as shown in Figure 1.

This elongated C_{3v} effective symmetry raises a significant problem with respect to the present interpretations of the small copper hyperfine splitting observed in the blue copper EPR spectrum. The small splitting had been attributed¹⁰ to a D_{2d}

mixing of Cu $4p_z$ into the $d_{x^2-y^2}$ ground-state orbital. Electron spin in $4p_z$ would produce oppositely signed dipolar coupling with the nuclear spin than that arising from an electron in $d_{x^2-y^2}$. The two together would thus tend to cancel the anisotropic part of the hyperfine tensor. However, a C_{3v} distortion can only mix p_x and p_y with the $d_{x^2-y^2}$ orbital. These are of the same sign for dipolar coupling and thus would tend to increase the hyperfine splitting. Alternatively, other features of the ground-state wave function could also lead to a reduction of the hyperfine coupling constant. In particular, electron delocalization onto the ligands due to strong bonding interactions and low symmetry mixing with the $4s$ orbital on the Cu atom could be responsible.

Thus, these detailed single-crystal spectral studies on plastocyanin raised important questions concerning the electronic structure and bonding at the blue copper site. In this paper, we address these questions through self-consistent field- $X\alpha$ -scattered wave (SCF- $X\alpha$ -SW) calculations. In particular, we have focused on the nature of the short copper-thiolate bond, on the long copper-thioether bond, and on a theoretical and experimental description of the ground-state wave function.

II. Details of the Calculation and Experimental

Standard versions of spin-restricted SCF- $X\alpha$ -SW calculations¹¹ were performed on the IBM 3081 and 3033 computers at the Stanford Linear Accelerator Center. In order to satisfy the limitations imposed by the dimensions of the scattered wave programs, various approximations as to the nature of ligands and symmetry in the blue copper site were used. Thus, calculations were performed on four versions of the site (bottom, Figure 1).

In the principal approximation to the site, the imidazole rings of histidine 37 and 87 were replaced by ammonia, methanethiolate was substituted for the thiolate side chain of cysteine 84, and methionine 92 was replaced by dimethyl thioether. The ligands in this site (designated $C_s(\text{met})$) were rearranged slightly to an idealized geometry with a plane of symmetry containing the carbon, sulfur, and copper nuclei and bisecting both the N-Cu-N and the thioether C-S-C angles. The N-Cu bond distances were averaged to 2.07 Å, and the N-Cu-N bond angle was 97° . To evaluate specific features of this approximation, as well as to understand the effect of variation in ligand at the site, calculations were performed on three other variants of the blue copper site.

In the first of these, the effect of thioether coordination was evaluated by its removal from the $C_s(\text{met})$ site. This new site (C_s) was identical with the $C_s(\text{met})$ site with the exception of the elimination of the thioether. In the second approximation, the effect of lowered symmetry was evaluated. Here, the mirror plane of the C_s site was removed and the real plastocyanin coordinates⁵ were used. Due to dimensional constraints, this site approximation lacked thioether coordination. The amines of the C_s calculation were replaced with imidazoles in the fourth approximation to the blue site to evaluate the effect of histidine coordination. This site ($C_s(\text{his})$) also required the replacement of the thiolate with HS⁻.

A complication occurred in the $C_s(\text{his})$ calculation: with integral occupation numbers, the calculation always converged with filled orbitals higher in energy than the half-filled orbital. Two approaches yielding similar results were taken to solve this problem. In the first approach, non-integral occupancy was allowed between the two energy levels involved and the occupancy was varied until these partially occupied levels became degenerate to within 88 cm^{-1} . When the orbital $16a''$, which is largely of copper d and sulfur p character, had an occupancy of 1.33 electrons and the orbital $15a''$, which is an antisymmetric combination of orbitals on the two imidazole rings, was occupied by 1.67 electrons, the calculation converged with the filled levels below all of the partially filled levels.¹² The second approach involved a transition-state-type calculation in which the occupation numbers of both the $15a''$ and $16a''$ levels are set to 1.5 electrons and the potential is converged. Here, the level $15a''$ has an energy eigenvalue 0.28 above that of $16a''$. This result again suggests that $16a''$ should be regarded as the half-filled orbital.¹³

(7) Penfield, K. W.; Gay, R. R.; Himmelwright, R. S.; Eickman, N. C.; Norris, V. A.; Freeman, H. C.; Solomon, E. I. *J. Am. Chem. Soc.* **1981**, *103*, 4382-4388.

(8) Thamann, T. J.; Frank, P.; Willis, L. J.; Loehr, T. M. *Proc. Natl. Acad. Sci. U.S.A.* **1982**, *79*, 6306-6400.

(9) Scott, R. A.; Hahn, J. E.; Doniach, S.; Freeman, H. C.; Hodgson, K. O. *J. Am. Chem. Soc.* **1982**, *104*, 5364-5369.

(10) (a) Bates, C. A.; Moore, W. S.; Standley, K. J.; Stevens, K. W. H. *Proc. Phys. Soc.* **1962**, *79*, 73-83. (b) Roberts, J. E.; Brown, T. G.; Hoffman, B. M.; Peisach, J. *J. Am. Chem. Soc.* **1980**, *102*, 825-829.

(11) (a) Johnson, K. H. *Adv. Quantum Chem.* **1973**, *7*, 143. (b) Johnson, K. H.; Norman, J. G., Jr.; Connolly, J. W. D. In "Computational Methods for Large Molecules and Localized States in Solids"; Herman, F., McLean, A. D.; Nesbet, R. K., Eds.; Plenum: New York, 1973. (c) Connolly, J. W. D. In "Semiempirical Methods of Electronic Structure Calculation, Part A: Techniques"; Segal, G. A. Ed.; Plenum: New York, 1977. (d) Rosch, N. In "Electrons in Finite and Infinite Structures"; Phariseau, L.; Scheire, L., Eds.; Plenum: New York, 1977. (e) Slater, J. C. "The Calculation of Molecular Orbitals"; Wiley: New York, 1979.

(12) (a) Slater, J. C. *Phys. Rev.* **1951**, *81*, 385. (b) Johnson, K. H., personal communication.

(13) Case, D. A., personal communication.

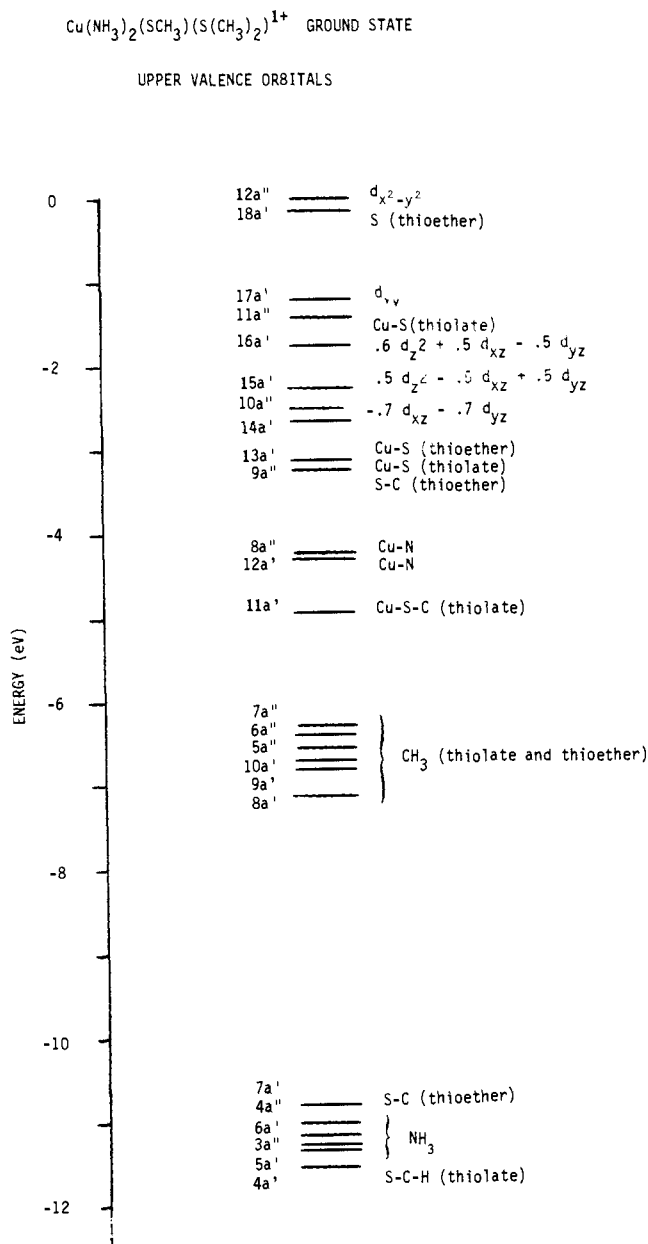


Figure 2. Highest occupied valence orbitals of $\text{Cu}(\text{S}(\text{CH}_3)_2)(\text{SCH}_3)(\text{NH}_3)_2^{1+}$ in the ground state. Energy of the highest occupied level set to zero.

In the results that we present, the $16a''$ level was given an occupation number of 1. An analogous problem occurred in Case and Karplus' study of copper porphine.¹⁴

The positions of the atoms, sphere radii, α values, and maximum values for the azimuthal quantum number 1 for the C_r (met) and C_1 calculations were given in Table I. The α values used were those determined by Schwarz.¹⁵ The Norman criteria¹⁶ were used to determine the sphere sizes. A Watson sphere of equal but opposite charge was used in all calculations of charged species. The calculations were considered converged when the largest relative change in the potential between subsequent iterations was less than 0.01.

For comparison, calculations were performed on the free ligands involved in ligation at the site. These included methanethiol,¹⁷ methanethiolate, dimethyl sulfide,¹⁸ and imidazole.¹⁹ Input coordinates for these compounds were taken from the literature.

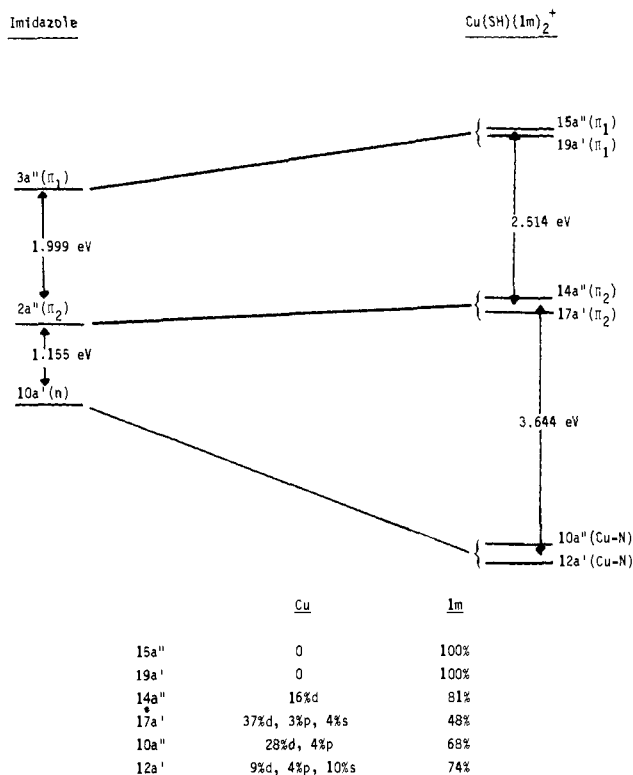


Figure 3. Interaction of the three highest energy occupied orbitals of imidazole with copper. Top: shifts in energy (brackets identify symmetric and antisymmetric combinations of similar orbitals on the two imidazole rings in the complex). Bottom: imidazole and copper character of the orbitals.

Plastocyanin was obtained from spinach leaves and isolated according to the method of Borchert and Wessels.²⁰ Q-band EPR spectra were obtained on a Bruker ER-220D spectrometer equipped with a 051 QR bridge and a variable-temperature attachment which maintained samples at 100 K. Spectra were calibrated with DPPH, and parameters were extracted by simulating powder spectra and varying the values of g and A until no further improvement was possible.

III. Results and Discussion

A. Blue Copper Site Model Calculations. The energies and charge decompositions resulting from $X\alpha$ calculations on the four approximations to the blue copper active site are shown in Table II. Figure 2 shows an energy level diagram of the C_r (met) site.

The results of the C_r (his) calculation are best understood by first considering the ground-state $X\alpha$ calculation of free imidazole which is given in Figure 3. Like calculations have been performed by Case et al.²¹ with different sphere radii and l values but with similar results. The three highest energy orbitals, $3a''$, $2a''$, and $10a'$, are referred to in the literature²² as π_1 , π_2 , and n , respectively. The orbitals π_1 and π_2 are delocalized over the ring, while the n orbital contains a lone pair of electrons localized on a nitrogen atom. The calculated (transition state) and experimentally determined ionization energies from these levels are compared in Table III. The agreement between theory and experiment is quite good for the first two levels while some discrepancy exists for the n orbital, as this level is calculated 1.8 eV above what is experimentally observed.

A comparison of the π_1 , π_2 , and n levels in free imidazole with the corresponding levels in the copper complex is shown in Figure 3. Note that in the complex, molecular orbitals consisting of symmetric (a') and antisymmetric (a'') combinations of each set

(14) Case, D. A.; Karplus, M. *J. Am. Chem. Soc.* **1977**, *99*, 6182.

(15) Schwartz, K. *Phys. Rev. B* **1972**, *5*, 2466.

(16) Norman, J. G., Jr. *Mol. Phys.* **1976**, *31*, 1191.

(17) Kojima, J.; Nishikawa, T. *J. Phys. Soc. Jpn.* **1957**, *12*, 680.

(18) The same coordinates as those of the thioether ligand in plastocyanin were used.

(19) Ha, T.-K. *Chem. Phys. Lett.* **1976**, *37*, 315.

(20) Borchert, M. T.; Wessels, J. S. C. *Biochem. Biophys. Acta* **1970**, *197*, 78.

(21) Case, D. A.; Cook, M.; Karplus, M. *J. Chem. Phys.* **1980**, *73*, 3294.

(22) (a) Fawcett, T. G.; Bernarducci, E. E.; Krogh-Jespersen, K.; Schugar, H. J. *J. Am. Chem. Soc.* **1980**, *102*, 2598. (b) Schugar, H. J. In "Copper Complexation Chemistry: Biochemical and Inorganic Perspectives"; Karlin, K. D.; Zubieta, J., Eds.; Adenine: Gunderland, N.Y., 1983; p 43.

Table I. Input Parameters for $C_s(\text{met})$ and C_1 Calculations

atom	position			radius	α	l_{max}
	x	y	z			
A. $C_s(\text{met})$: $\text{Cu}(\text{S}(\text{CH}_3)_2)(\text{SCH}_3)(\text{NH}_3)_2^+$						
outer sphere	0.0	0.0	0.0	10.6849	0.79626	3
Cu	0.0	0.0	0.0	2.5589	0.70697	2
S(methionine)	-0.5064	-5.4632	0.0	2.3600	0.72475	1
S(cysteine)	3.8928	1.0318	0.0	2.4390	0.72475	1
C(cysteine)	5.8052	-1.7537	0.0	1.7695	0.75928	1
HCA(cysteine)	4.5807	-3.4147	0.0	1.2900	0.97804	0
HCB(cysteine)	6.9920	-1.7590	± 1.6875	1.2930	0.97804	0
N(amine)	-2.5757	0.4195	± 2.9121	1.7138	0.75197	1
HNA(amine)	-1.5930	0.4195	± 4.5429	1.1771	0.97804	0
HNB(amine)	-3.4733	2.0768	± 2.6381	1.1772	0.97804	0
HNC(amine)	-3.7813	-1.0488	± 2.8195	1.1760	0.97804	0
C(methionine)	1.0771	-7.0789	± 2.6305	1.7605	0.75928	1
HC1(methionine)	0.3779	-6.3665	± 4.3672	1.2674	0.97804	0
HC2(methionine)	0.7124	-9.0461	± 2.5209	1.2671	0.97804	0
HC3(methionine)	3.0500	-6.7558	± 2.5209	1.2657	0.97804	0
B. C_1 : ^a $\text{Cu}(\text{SCH}_3)(\text{NH}_3)_2^+$						
outer sphere	0.0	0.0	0.0	8.6981	0.78962	3
Cu	0.0	0.0	0.0	2.5693	0.70697	2
S	3.8928	1.0318	0.0	2.4392	0.72475	1
C	5.8052	-1.7537	0.0	1.7698	0.75928	1
HCA	4.5807	-3.4147	0.0	1.2930	0.97804	0
HCB	6.9920	-1.7590	1.6880	1.2932	0.97804	0
HCC	6.9920	-1.7590	-1.6880	1.2932	0.97804	0
N1 (his 87)	-2.4400	0.8010	8.0310	1.7157	0.75197	1
HNA	-1.3889	0.8010	4.6200	1.1778	0.97804	0
HNB	-3.2088	2.5110	2.7020	1.1769	0.97804	0
HNC	-3.7640	-0.5670	3.0690	1.1772	0.97804	0
N2 (his 37)	-2.6820	0.0490	-2.7550	1.7129	0.75197	1
HND	-1.7730	0.0490	-4.4300	1.1779	0.97804	0
HNE	-3.7470	-1.5160	-2.5360	1.1778	0.97804	0
HNF	-3.7100	1.6350	-2.5170	1.1773	0.97804	0

^a Atom positions from ref 5.

of imidazole orbitals are found. The antisymmetric-symmetric splitting is 0.088 eV for the π_1 set, 0.226 eV for the π_2 set, and 0.267 eV for the n levels. The average splitting between the π_1 and π_2 , and π_2 and n orbitals is calculated to increase upon complexation, going from 1.999 to 2.514 and 1.555 to 3.644 eV, respectively. Note that the splitting between the nonbonding π_1 and the π interacting π_2 levels increases less than the splitting between the π_2 and n levels where the latter are involved in σ bonding with the copper. In addition, the orbitals 15a'' and 19a' (the π_1 set) have no copper character while 14a'' has some copper character and 17a' has substantial copper character. This level mixes dominantly with the d_{xz} orbital and, since the π levels are not present in calculations with amine, leads to a significant reduction in Cu d character in the 16a' level of $C_s(\text{his})$ relative to the 16a' level in the $C_s(\text{met})$ calculation. A further comparison between the $C_s(\text{met})$ and $C_s(\text{his})$ calculations indicates that the addition of imidazole contributes little to the already limited mixing between the thiolate and imidazole valence levels and that the character of the ground state does not change substantially. Thus, the $C_s(\text{met})$ calculation can be viewed as a reasonable representation of the actual blue copper active site in plastocyanin.

B. Copper-Thiolate Interaction. The highest energy occupied valence energy levels of the ground state of methanethiolate are shown in Figure 4, left. The highest energy level, 2e (in C_{3v} symmetry), is a doubly degenerate orbital of almost entirely sulfur p_x and p_y character. To 2.2 eV deeper binding energy the $3a_1$ level has 59% sulfur p_z character; it is this orbital which forms the σ bond between the sulfur atom and the methyl group. Note that while this is formally an sp_2 hybrid orbital on the sulfur, it contains only 2% s character due to the 7.448 eV deeper binding energy of the 3s level. These valence levels are the ones involved in the formation of bonds between the thiolate sulfur and the copper site.

Coordination of a proton to methanethiolate at an angle less than 180° splits the 2e and $3a_1$ levels into three nondegenerate orbitals. The results of a transition-state calculation on meth-

anethiol, with the proton at 96° relative to the S-C axis, are given in Table III. Experimental ionization energies are also given. The agreement is quite good between the theoretical and experimental values of the two lowest ionization energies. The ionization energy of the third level, however, is calculated at approximately 1.3 eV higher than is experimentally observed.

The nature of the interaction between methanethiolate and a copper atom is further complicated due to the presence of the valence d orbitals on the metal ion (see Figures 4 and 5). In Figure 4 the thiolate valence orbitals split into three nondegenerate levels due to strong bonding interactions with the copper. All three levels show significant electron delocalization onto the copper (7a'', 42%; 9a', 45%; 7a', 21%). These are separated by 1.6 and 2.1 eV in the ground state and 1.6 and 1.9 eV in the transition-state calculation. On the basis of the comparison of the thiol $X\alpha$ calculations to the UPS experimental results (Table III), one might expect the calculated thiolate valence orbital splitting for the blue copper site in Figure 4 to overestimate the experimental value by ≈ 1.5 eV. The components of the 2e level split upon copper coordination. The out-of-plane component, 7a'', forms a π bond with the copper $d_{x^2-y^2}$ orbital (see Figure 5, top right frame). The in-plane component is stabilized and mixes considerably with the $3a_1$ orbital; two in-plane (C-S-Cu) bonds result (middle and bottom frames, Figure 5). The higher of these two orbitals (9a') is localized primarily around the copper and sulfur nuclei, with only 10% methyl character. This is best described as a pseudo- σ -type bond in that the maximum of electron density is not localized along the Cu-S axis. The orbital at deepest binding energy (7a') should be viewed as a molecular orbital significantly delocalized over the Cu-S-C bond with 31% methyl character. This S-C bonding interaction appears to stabilize the 7a' orbital relative to level 9a'.

Thus, the blue copper site possesses three bonding molecular orbitals (one π and two σ) approximately equally split in energy, with significant sulfur and copper character. All three molecular orbitals have substantial sulfur 3p character and almost no sulfur

Table II. Results of SCF-X α -SW Calculations on C_r(met), C₁, C_s, and C_s(his) Sites

		C _r (met)										
		charge distribution (%)										
level ^a	orbital	energy (eV)	Cu			S(cysteine)		N		S(methionine)		
			s	p	d	s	p	s	p	s	p	
ligand field	12a'' ^b	-6.444		1	31			41	1	10		
	17a'	-7.643	4	8	46			23	1	4		2
	16a'	-8.206	2		51	1	4		4			19
	15a'	-8.686	1		77		6		1			6
	10a''	-8.914			93		3					
thiolate	11a''	-7.862		7	28			28	1	18		
	13a'	-9.562		2	45	2	33		3			1
	11a'	-11.370	11	1	13		36			10		
amine	8a''	-10.676		3	47			1	2	38		
	12a'	-10.736	6	5	21		13	1		36		
thioether	18a'	-6.593		1	7			2				65
	14a'	-9.099	3		29		3				1	35
		C ₁										
		charge distribution (%)										
level	orbital	energy (eV)	Cu			S		N ₁ ^c		N ₂ ^c		
			s	p	d	s	p	s	p	s	p	
ligand field	20a ^b	-5.828		1	33			37	1	6		5
	19a	-6.876	4	7	46			25		5		1
	17a	-7.705	3	1	73	1	9		1			2
	16a	-8.004	2		89		2		1			1
	15a	-8.198			93		3					
thiolate	18a	-7.246		6	28			30		7	1	9
	14a	-8.816		1	45	2	33		1			1
	11a	-10.594	11	1	14		31		2			12
amine	13a	-9.805	4	3	42			2	2	38		
	12a	-10.068	1	5	29		16				1	31
		C _s										
		charge distribution (%)										
level	orbital	energy (eV)	Cu			S			N			
			s	p	d	s	p	d	s	p		
ligand field	8a'' ^b	-5.636		1	32			39			1	11
	12a'	-6.695	4	7	48			25				4
	11a'	-7.600	4	1	75	1	5		1			4
	10a'	-7.810			91		2		1			1
	6a''	-7.994			91		4					1
thiolate	7a''	-7.106		7	30			28			1	16
	9a'	-8.682		2	41	3	35		1			3
	7a'	-10.730	10	2	13	1	33		3			6
amine	5a''	-9.746		3	46			1			2	38
	8a'	-9.823	7	5	20	1	3				2	40
		C _s (his)										
		charge distribution (%)										
level	orbital	energy (eV)	Cu			S		N				
			s	p	d	s	p	s	p			
ligand field	16a'' ^b	-7.518			34			46	1			5
	18a'	-8.355	3	4	42			15				13
	16a'	-9.308	3		87			2				2
	15a'	-9.638			76			2				4
	12a''	-9.684			86			4				2
thiolate	13a''	-9.083	2		38			24		2		11
	14a'	-10.634	1	3	38	4	45					
	11a'	-14.226	5	4	8	6	53					
π_1	15a''	-6.046										100 (π_1)
	19a'	-6.134										100 (π_1)
π_2	14a''	-8.491			13			2				64 (π_2)
	17a'	-8.717	3	3	31			7				40 (π_2)
n	10a''	-12.115		4	27					4		36
	12a'	-12.382	9	4	8	1	2			4		37

^aRefers to principle character of orbital. Only upper valence orbitals are given. ^bHalf-occupied orbital. ^cN₁ is the nitrogen of his(87).

Table III. Experimental and Theoretical Ionization Energies

level	X α (eV)	exptl (eV)
Dimethyl Sulfide		
2b ₂	8.43	8.65 ^a
4a ₁	10.58	11.2 ^a
3b ₁	11.84	12.6 ^a
Imidazole		
3a''	8.22	8.8 ^b
2a''	10.46	10.3 ^b
10a'	12.08	10.3 ^b
Methanethiol		
2a''	9.15	9.42 ^a
5a'	11.81	12.0 ^a
4a'	15.17	13.9 ^a

^aFrost, D. C.; Herring, F. G.; Katrib, A.; McDowell, C. A.; McLean, R. A. N. *J. Phys. Chem.* **1972**, *72*, 1036. ^bCradock, S.; Findlay, R. H.; Palmer, M. H. *Tetrahedron* **1973**, *29*, 2173.

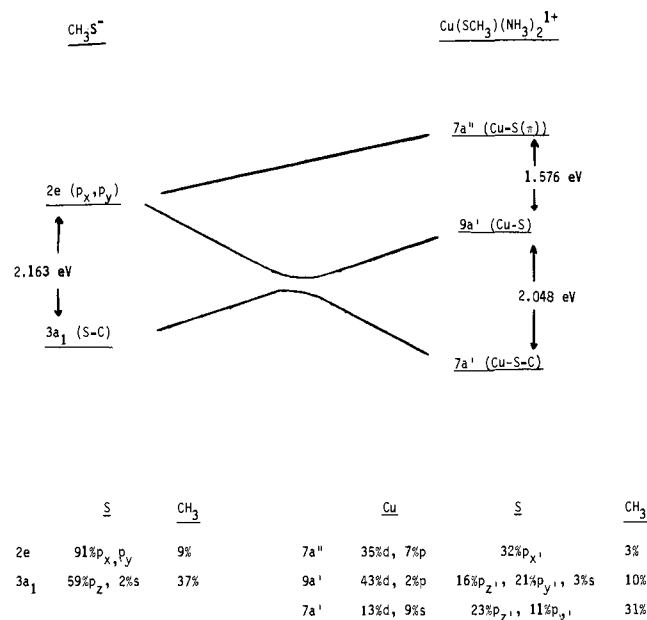


Figure 4. Interaction of the three highest energy orbitals of methanethiolate with a copper(II) ion. Top: shifts in energy (relative to the sulfur 2s orbital). Bottom: character of the orbitals in terms of atomic orbitals. Primed coordinates of the copper-bound sulfur p orbitals indicate a ligand-based coordinate system.

3s character. Finally, very little interaction of these levels with other ligands was observed.

C. Copper-Thioether Interaction. The relative energies of the three highest valence orbitals of the ground state of dimethyl sulfide are given in Figure 6, left. The highest energy orbital, 2b₂, is largely of out-of-(C-S-C)plane sulfur p_y' character. The next two orbitals, 4a₁ and 3b₁, form sulfur-carbon bonds with symmetric and antisymmetric combinations of methyl orbitals. The sulfur character in both of these molecular orbitals comes primarily from in-plane p orbitals. Again, little 3s hybridization on the sulfur is observed due to its significantly deeper binding energy (8.171 eV). The agreement between experimentally observed ionization energies from these levels and ionization energies calculated for transition states is quite good (see Table III).

Figure 6 depicts the changes which occur in the three highest energy thioether orbitals when the thioether ligand interacts with the blue copper site at a distance of 2.9 Å. The decompositions and splittings in energy of the first and third levels (2b₂ and 3b₁ in the free ligand, 18a' and 9a'' in the complex) are nearly the same for the free and bound ligand. However, the second level (4a₁ in the free ligand, 14a' in the complex) is stabilized in energy relative to the other two levels and acquires considerable metal character (36%) upon interaction with the copper ion. A contour diagram of the 14a' level of the blue copper complex (C_s(met))

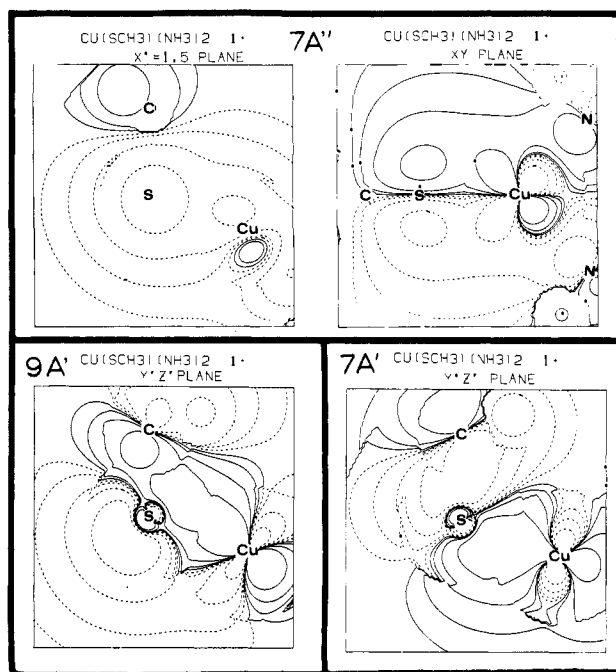
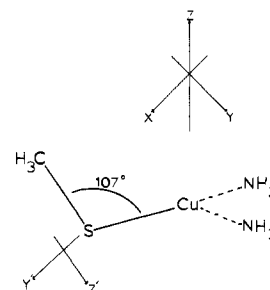


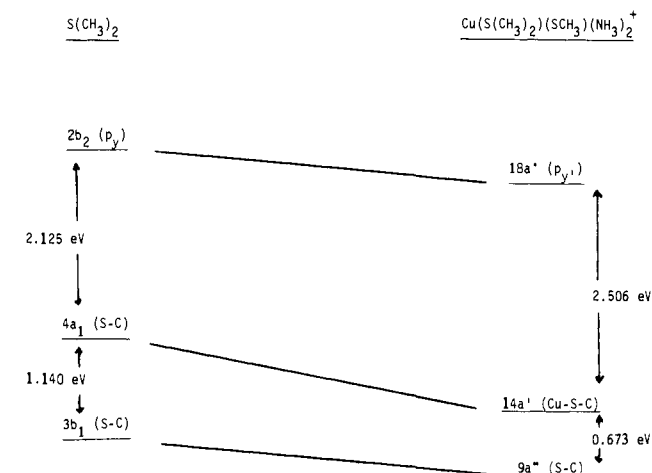
Figure 5. Contours of the three bonding orbitals with substantial thiolate sulfur 3p character and the geometry of Cu(SCH₃)(NH₃)₂⁺ with copper- and thiolate-based coordinate systems indicated. All nuclei indicated are in the planes of the figures except for the contour of the 7a'' orbital in the xy plane. Only the copper nucleus is in the plane of this figure. Values of the contours are ±0.003, ±0.009, ±0.027, and ±0.081.

is presented in Figure 7. The diagram demonstrates that the 14a' wave function results from a pseudo-σ-bonding interaction (the maximum electron density not being directly along the Cu-S axis) between the sulfur p_z orbital on the thioether and the d_z orbital on the copper. It should be noted that while the tilt of approximately 50° of the thioether plane relative to the Cu-S axis results in a slightly better orientation of the sulfur p_y' orbital of the 2b₂ wave function of the thioether for bonding with the copper orbitals, the closeness in energy of the thioether 4a₁ level and the copper d_z orbital produces the primary bonding interaction between the metal and this ligand.

The effect of the axial thioether upon the SCF-X α -SW calculated energies of the copper d orbitals is presented in Figure 8. Here, the relative calculated energies of the copper d orbitals are given for the copper site in C_s symmetry with and without the thioether. Upon addition of the axial ligand, three of the four levels go down slightly in energy relative to the half-occupied level. The d_z level, however, goes up in energy due to antibonding interactions with the sulfur p_z orbital of the thioether. Thus the d-d transition associated with the d_z orbital should go down in energy. While experimentally removing the thioether from a blue copper site and at the same time retaining the remaining geometric features is unrealistic, copper chloride spectral analogue studies^{23,24} do clearly demonstrate destabilization of the d_z orbital due to antibonding interactions with chloride ligands at approximately 3 Å as shown in Figure 9. At the top of the figure is the lig-

(23) Hitchman, M. A.; Cassidy, P. J. *Inorg. Chem.* **1978**, *17*, 1682.

(24) Hitchman, M. A.; Cassidy, P. J. *Inorg. Chem.* **1979**, *18*, 1745.



	S	CH ₃		Cu		S	CH ₃
2b ₂	92% p _y	8%	18a'	6% d _{z²} , 2% d _{xy}	80% p _y	6%	
4a ₁	64% p _z , 3% s	31%	14a'	28% d _{z²} , 5% d _{xy} , 3% s	39% p _z , 1% s	18%	
3b ₁	47% p _x	48%	9a''	1% d	55% p _x	44%	

Figure 6. Interaction of the three highest energy occupied orbitals of dimethyl sulfide with copper. Top: shifts in energy (relative to the sulfur 2s orbital). Bottom: character of the orbitals in terms of atomic orbitals. Primed coordinates of the copper-bound sulfur p orbitals indicate a ligand-based coordinate system.

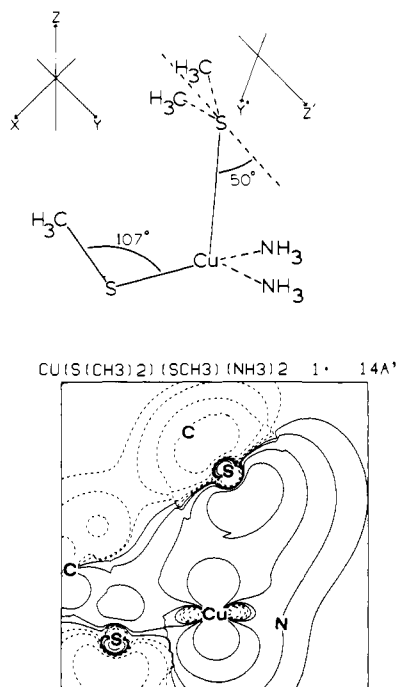


Figure 7. Contour of the 14a' level and the geometry of Cu(S(CH₃)₂)(SCH₃)(NH₃)₂⁺ with copper- and thioether-based coordinate systems indicated. In the contour, all nuclei indicated are in the plane of the diagram except for those of the amine nitrogens and thioether carbons. Values of the contours are the same as in Figure 5.

and-field spectrum of bis(*N*-methylphenethylammonium)CuCl₄ [(nmph)₂CuCl₄], which contains no axial ligand. At the bottom is the spectrum of bis(ethylammonium)CuCl₄ which does contain axial chlorides. The assigned transitions for each complex are indicated at the top of the absorption bands in Figure 9. Upon addition of the apical chlorides (Figure 9, top → bottom), the transition from the d_{z²} orbital decreases in energy from 16 000 to 11 000 cm⁻¹, while the other transitions occur at approximately

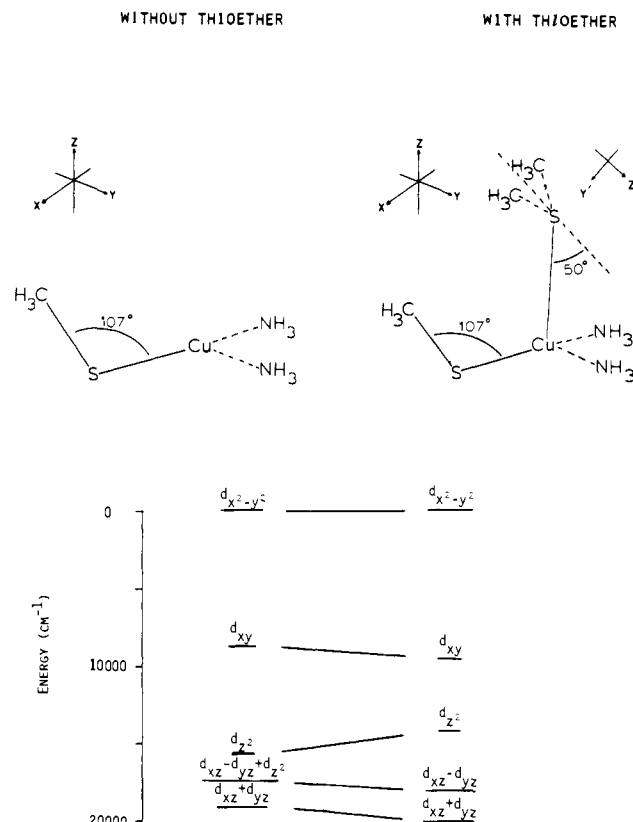


Figure 8. Calculated effects of axial thioether ligation upon copper d orbitals. The relative energies of the antibonding orbitals and their predominant copper d character are indicated for the two sites shown. The energies of the half-occupied levels have been set to zero.

the same energies in both complexes. Thus, a distant apical ligand has significant effect upon the energy of the d_{z²} orbital of the complex.

To summarize this section, the 4a₁ (sulfur p_z) orbital in the axial thioether would appear to undergo a small but significant bonding interaction with the d_{z²} orbital on the copper as shown in Figure 8. This interaction is found to significantly affect the energy of the d_{z²} → d_{x²-y²} ligand-field transition. A complete evaluation of this effect in plastocyanin must await a detailed analysis of MCD and absorption features in the near-IR spectral region.

D. Ground State Wave Functions. (i) g Values. To a first approximation, the ground state of plastocyanin, referred to earlier as the d_{x²-y²} orbital, can be taken directly from the 12a'' level of the C_s calculation or the 20a level in the C₁ site presented in Table II. A significant feature of these levels is the large contribution of the sulfur 3p orbitals, indicating that the ground state is very covalent. While some delocalization must occur, the magnitude apparent here is quite large, making it important to consider the performance of these calculations with regard to delocalization. It is apparent from many Xα-SW studies that the multiple scattering formalism overestimates the amount of ligand character in the ground state wave function.²⁵ Thus, an experimental estimate of the amount of covalent delocalization is required before a reasonable approximation to the ground state can be obtained. The ground-state parameters most sensitive to delocalization are the EPR g and superhyperfine coupling values. In plastocyanin, however, the delocalization occurs primarily over the sulfur p orbitals. As only ³³S (natural abundance 0.76%) has nonzero nuclear spin among naturally occurring sulfur isotopes, no superhyperfine from the sulfur in plastocyanin is observed. Any experimental fit of the ground state wave function must therefore be made to EPR g values.

(25) (a) Sontum, S. F.; Case, D. A. *J. Phys. Chem.* **1982**, *86*, 1596. (b) Cook, M. R. Ph.D. Thesis, Harvard University, 1981. (c) Sunil, K. K.; Rodgers, M. *Inorg. Chem.* **1981**, *20*, 3283.

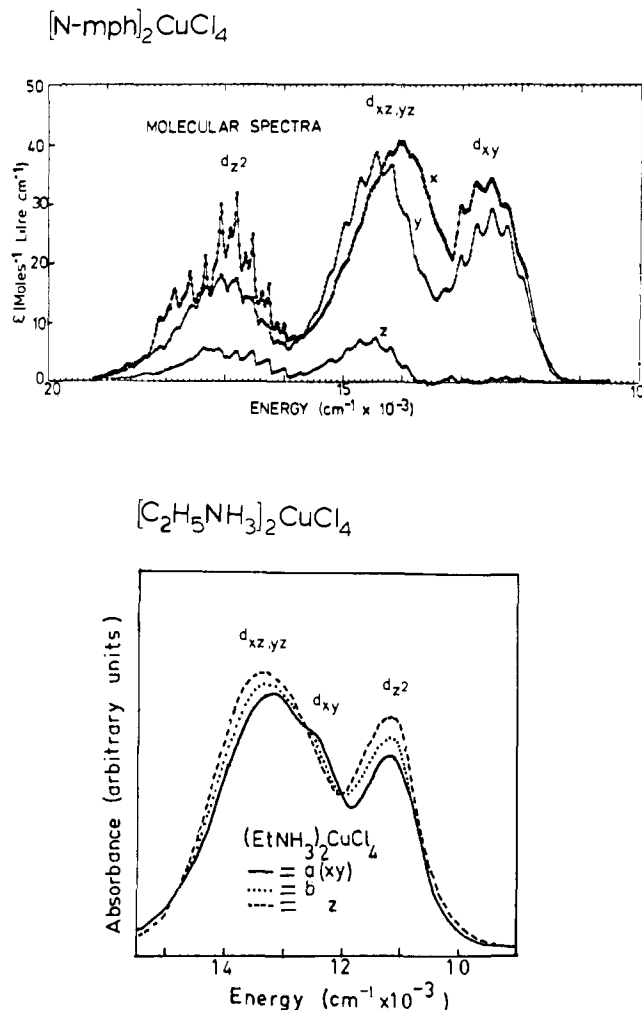


Figure 9. Top: molecular spectrum of the planar CuCl_4^{2-} ion in $(\text{nmph})_2\text{CuCl}_4$. Adapted from ref 24. Bottom: molecular spectrum of the tetragonal copper site in bis(ethylammonium) CuCl_4 . Adapted from ref 23. Polarization and assignments are indicated in each figure.

Ideally, a completely empirical fit of the ground state wave function to the experimental g values would give covalent delocalizations without the intervening approximations of a crystal field or $X\alpha$ bonding theory. However, even the relatively simple second-order perturbation formalism²⁶ requires the knowledge of both excited- and ground-state delocalizations to obtain a g value. Thus, a completely empirical fit to even an isotropic EPR spectrum will be underdetermined. One approach to this problem has been to use Steven's orbital reduction factors²⁷ in place of explicit expressions for the metal and ligand contribution to the wave function. However, the interpretation of these factors is at best uncertain, and their relation to covalent delocalization is complicated.²⁸

The starting point for our calculation of ground-state parameters was the partitioned-charge decomposition of the converged $X\alpha$ calculation.²⁹ As this charge decomposition does not form a complete set of wave functions, the Gram-Schmidt technique was used to generate an orthonormal set of basis functions. In this

step, the one-electron wave functions were orthogonalized in order of increasing energy so that the lowest energy functions, which have the greatest influence in the calculation of ground-state parameters, were changed the least. Thus, the ground state is not changed by this procedure. A matrix of states was established by using the orthonormalized functions, electron spin was included, and spin-orbit coupling was evaluated. This complete calculation avoids any inaccuracies which may arise in the perturbation expressions when low-lying excited states are mixed into the ground state with large spin-orbit coupling constants. As with perturbation methods which include both metal and ligand character explicitly,^{30,31} spin-orbit coupling is evaluated separately over both sets of centers.³² Consistent with the scattered-wave solution to the $X\alpha$ problem, overlap integrals between metal- and ligand-centered orbitals and between ligands on different centers were set strictly to zero. A matrix element M_{ij} between two states ψ_i and ψ_j would thus have the form

$$M_{ij} = E_{ij}\delta_{ij} + \langle \psi_i | \lambda L \cdot S | \psi_j \rangle \quad (1)$$

Here, the diagonal elements E_{ii} are energies and the ψ_i are expressed as

$$\psi_i = \sum_{j=1}^5 a_{ij}\chi_j + \sum_{j=6}^n b_{ij}\phi_j \quad (2)$$

where the χ_j and the d orbitals and ϕ_j are other metal-centered and ligand orbitals. If there are m states, the dimension of M after the addition of spin is thus $2m$ by $2m$. The spin-orbit coupling constants³³ used in calculating the off-diagonal elements were $\lambda_{\text{Cu}} = -828 \text{ cm}^{-1}$, $\lambda_{\text{S}} = -382 \text{ cm}^{-1}$, and $\lambda_{\text{N}} = 76 \text{ cm}^{-1}$. While there is some evidence³⁴ to suggest that the spin-orbit coupling parameter of copper does not change significantly from the free ion value with increasing delocalization, such evidence is lacking for sulfur. However, varying this number by several tens of wavenumbers produced relatively minor changes in the calculated g values. Thus, the free-atom value was used. Diagonalizing the matrix gave spin-orbit corrected energies and spin-orbit corrected wave functions. The original input energies, E_{ii} , were then adjusted until the spin-orbit corrected energies corresponded with what was experimentally observed. The spin-orbit corrected ground state was used to calculate a g^2 tensor by using an approach outlined by Gerloch and McMeeking.³⁵ For a general matrix element g^2_{ij} (where $i, j = x, y, z$), we have

$$g^2_{ij} = 2 \sum_{\alpha, \beta} \langle \alpha | \mu_i | \beta \rangle \langle \beta | \mu_j | \alpha \rangle \quad (3)$$

where the sum is over both parts α and β of the Kramers doublet ground state wave function and μ_i represents the Zeeman operator $L_i + 2.0023S_i$. Note that this approach makes no assumptions about symmetry. The g^2 tensor was diagonalized and the principal g values were obtained as the square root of the eigenvalues. The eigenvectors of this diagonalization represent the direction cosines of the diagonal g^2 tensor with respect to the orientation of the original basis set.

To test this approach on a simple high-symmetry complex, we determined the g values from our calculation of $D_{4h}\text{CuCl}_4$ ³⁶ using $\lambda_{\text{Cl}} = -587 \text{ cm}^{-1}$. The $X\alpha$ results gave $g_{\parallel} = 2.144$, $g_{\perp} = 2.034$,

(26) (a) Ballhausen, C. J. "Introduction to Ligand Field Theory"; McGraw-Hill: New York, 1961. (b) Smith, D. W. *J. Chem. Soc. A* 1969, 2529. (c) Smith, D. W. *J. Chem. Soc. A* 1970, 2900.

(27) Stevens, K. W. H. *Proc. R. Soc. London A* 1954, 226, 96.

(28) Gerloch, M.; Miller, J. R. *Prog. Inorg. Chem.* 1968, 10, 1-47.

(29) The most appropriate way to calculate g values from the output of an $X\alpha$ calculation would be to evaluate the operators $\partial/\partial i$ ($i = x, y, z$) over the output potential mesh since $L_x = -i\hbar(y(\partial/\partial z) - z(\partial/\partial y))$, etc. This would avoid the inconvenience and inaccuracy of having to assume a basis set for the wave function after completion of the calculation. However, such a calculation is difficult because the radial $X\alpha$ partitioned-charge functions are discontinuous at the sphere boundaries. In addition, there is no satisfactory method of expanding such operators about an arbitrary origin.^{25b}

(30) (a) McGarvey, B. R. In "Transition Metal Chemistry"; Carlin, R. L., Ed.; Marcel Dekker, Inc.: New York. (b) Maki, A. J.; McGarvey, B. R. *J. Chem. Phys.* 1958, 29, 31.

(31) (a) Smith, D. W. *J. Chem. Soc. A* 1970, 3108. (b) Bencini, A.; Gatteschi, D.; Zanchini, C. *J. Am. Chem. Soc.* 1980, 102, 5234. (c) Sharnoff, M. *J. Chem. Phys.* 1965, 42, 3383-3395. (d) Kivelson, D.; Neiman, R. *J. Chem. Phys.* 1961, 35, 149.

(32) Meistich, A. A.; Buch, T. *J. Chem. Phys.* 1964, 41, 2524.

(33) (a) Blume, M.; Watson, R. E. *Proc. R. Soc. London A* 1962, 271, 565.

(b) Keijzers, C. P.; deBoer, E. *Mol. Phys.* 1975, 29, 1007-20.

(34) Goodgame, B. A.; Rayner, J. B. *Adv. Inorg. Chem. Radiochem.* 1970, 13, 135.

(35) Gerloch, M.; McMeeking, R. F. *J. Chem. Soc., Dalton Trans.* 1975, 2443-51.

(36) Desjardins, S. R.; Penfield, K. W.; Cohen, S. L.; Musselman, R. L.; Solomon, E. I. *J. Am. Chem. Soc.* 1983, 105, 4590.

Table IV. Evaluation of Delocalization from Various Experimental Parameters and Techniques

parameter	complex	exptl value ($\times 10^{-4} \text{ cm}^{-1}$)	% metal character
A^{Cu} (hyperfine)	$\text{Cd}[\text{Cu}]\text{Cl}_2^a$	$A_{\parallel}^{\text{Cu}} = 113$ $A_{\perp}^{\text{Cu}} = 0$	70
	$\text{K}_2\text{Pd}[\text{Cu}]\text{Cl}_4^b$	$A_{\parallel}^{\text{Cu}} = 164$ $A_{\perp}^{\text{Cu}} = 34.5$	63
A^{Cl} (superhyperfine)	$\text{Cd}[\text{Cu}]\text{Cl}_2^a$	$A_{\parallel}^{\text{Cl}} = 18.5$ $A_{\perp}^{\text{Cl}} = 5.0$	64
	$\text{K}_2\text{Pd}[\text{Cu}]\text{Cl}_4^b$	$A_{\parallel}^{\text{Cl}} = 19.9 (23.3)^b$ $A_{\perp}^{\text{Cl}} = 7.0 (5.3)^b$	63 (49) ^b
UPS	$[(\text{CH}_3)_2\text{NH}_3]_2\text{CuCl}_4^c$		65

^a From ref 40. ^b From ref 39. In this reference the derived superhyperfine parameters $A_{\parallel}^{\text{Cl}}$ and A_{\perp}^{Cl} could not be obtained from the stated experimental parameters (shown in parentheses). Thus, we calculated $A_{\parallel}^{\text{Cl}}$ and A_{\perp}^{Cl} from $A_{\parallel}^{\text{Cu}}$ and A_{\perp}^{Cu} and evaluated delocalization using both sets of data. ^c From ref 41. Represents an average for all d orbitals.

while the experimental values³⁷ are $g_{\parallel} = 2.221 \pm 0.004$, $g_{\perp} = 2.040 \pm 0.004$. Since the calculated values are smaller than those obtained experimentally, it is apparent that the $X\alpha$ calculation overestimates the degree of delocalization.

In order to adjust for this overestimation of delocalization by the $X\alpha$ -SW formalism, we included a single parameter into the results of the calculation to adjust for differences between the calculated and the experimentally observed g values. The angular part of each level was retained, while the distribution of charge between the metal and ligands was adjusted from the initial $X\alpha$ output by the parameter Ω , which raises the amount of metal character and lowers the amount of ligand character in the antibonding ground level. The rest of the remaining levels were adjusted in proportion to the amount the metal character was raised in the ground state. Thus, if the amount of additional metal character in the ground state is Ω , the adjusted amount of metal character θ'_i in subsequent antibonding orbitals i and having θ_i percent metal character originally is

$$\theta'_i = (1 - \theta_i)\Omega / (1 - \theta_i) + \theta_i \quad (4)$$

in which θ_i is the original metal character of the ground state. For bonding levels, the corrected amount of metal character is given by

$$\theta'_i = \theta_i [1 - \Omega / (1 - \theta_i)] \quad (5)$$

Ligand character is adjusted in analogous fashion: antibonding orbitals lose ligand character, while bonding orbitals gain it. Ω was adjusted iteratively until satisfactory agreement with experimental g values was obtained. Application of this approach to D_{4h} CuCl_4^{2-} gives 64% metal character in the ground state with $g_{\parallel} = 2.221$, $g_{\perp} = 2.047$.

In order to test whether this 64% delocalization is reasonable and thus to check our method of calculation, we obtained additional estimates for the delocalization in D_{4h} CuCl_4^{38} using a variety of complementary experimental techniques. These results are presented in Table IV. Hyperfine delocalization was calculated according to the method of McGarvey.⁴² Here, the metal character (α^2) is obtained from

$$A_{\parallel} = P_d[-\kappa - \frac{1}{7}\alpha^2 + \Delta g_{\parallel} + \frac{3}{7}\Delta g_{\perp}] \quad (6a)$$

and

$$A_{\perp} = P_d[-\kappa + \frac{3}{7}\alpha^2 + \frac{1}{14}\Delta g_{\perp}] \quad (6b)$$

In this equation, $P_d (=g_e\beta_e g_N\beta_N / \langle r^3 \rangle_d)$ has the value of approximately $396 \times 10^{-4} \text{ cm}^{-1}$ (vide infra), Δg_{\parallel} and Δg_{\perp} are the ex-

perimental deviations from $g = 2.0023$, and κ is the indirect Fermi contact term. The simultaneous solution of eq 6a and 6b gives values for α^2 and κ . While this method does not correctly account for delocalization effects on the g values as they relate to the hyperfine expressions,⁴³ it gives an approximate estimate of 67% metal character for the ground state wave function. Similarly, ligand character was also calculated from the observed superhyperfine parameters $A_{\parallel}^{\text{Cl}}$ and A_{\perp}^{Cl} according to^{30b,34}

$$A_{\parallel}^{\text{Cl}} = (C_L)^2(1/4)[(n^2)A_{\text{iso}}^{\text{Cl}} + (1 - n^2)A_{\text{aniso}}^{\text{Cl}}] \quad (7a)$$

and

$$A_{\perp}^{\text{Cl}} = (C_L)^2(1/4)[(n^2)A_{\text{iso}}^{\text{Cl}} - \frac{1}{2}(1 - n^2)A_{\text{aniso}}^{\text{Cl}}] \quad (7b)$$

where C_L^2 is the percentage of ligand character, n^2 is the amount of 3s character mixed into the dominantly 3p ligand function, $A_{\text{iso}}^{\text{Cl}}$ is $\approx 1500 \times 10^{-4} \text{ cm}^{-1}$, and $A_{\text{aniso}}^{\text{Cl}}$ is $\approx 100 \times 10^{-4} \text{ cm}^{-1}$. The calculated ligand character in D_{4h} CuCl_4^{2-} from the simultaneous solution of eq 7a and 7b was 36%, implying a metal character of around 64%. Finally, we have used ultraviolet photoemission spectroscopy (UPS) to estimate the metal character of CuCl_4^{2-} averaged over the d orbitals to be $\approx 65\%$.⁴¹ While each of these methods is subject to different approximations, their consistency in yielding values in the 65% range lends support to our estimate through the fit of the $X\alpha$ calculation to the g values.

The delocalization adjustment used here gives ground-state delocalizations in good agreement with those determined from empirical calibration of hyperfine and superhyperfine values. However, it is important to compare this approach with alternative theoretical methods for determining mixing. Within the $X\alpha$ formalism, an approach exists to adjust the amount of ground-state delocalization relative to that obtained with use of the Norman criteria. Here, the sphere sizes are varied to empirically adjust the results of the calculation to experiment. A calculation⁴⁵ on D_{4h} CuCl_4^{2-} using this approach is available which enables the evaluation of empirical adjustment of sphere sizes. Increasing the overlap from 3% in our calculation to 13% increases the amount of ground-state mixing from 42% to 56%. The g values change from $g_{\parallel} = 2.144$, $g_{\perp} = 2.034$ to $g_{\parallel} = 2.206$, $g_{\perp} = 2.047$. It is apparent that increasing the sphere sizes and the amount of overlap moves the g values in the correct direction. However, the fit obtained by varying the sphere sizes gives somewhat more deviation from the experimental values of $g_{\parallel} = 2.221$, $g_{\perp} = 2.040$ than the present method of ground-state adjustment, which gave $g_{\perp} = 2.221$, $g_{\parallel} = 2.047$. A further consideration within the $X\alpha$ formalism involves the reapportionment of the charge in the inner-sphere region among the atomic spheres.⁴⁴ In our calculation, reapportioning the charge gave 46% metal character in the ground state of D_{4h} CuCl_4^{2-} and $g_{\parallel} = 2.144$, $g_{\perp} = 2.034$. However, if

(43) As is evident in our calculation of g values, delocalization onto ligands with non-trivial spin-orbit coupling constants can provide major contributions to the g values. In eq 6a and 6b, the terms Δg_{\parallel} and Δg_{\perp} take into account both ligand and metal contributions. In the calculation of metal hyperfine values, however, only metal centered components of the ground state wave function should be evaluated.

(44) Case, D. A.; Karplus, M. *Chem. Phys. Lett.* 1976, 39, 33.

(45) Bencini, A.; Gatteschi, D. *J. Am. Chem. Soc.* 1983, 105, 5535.

(37) Cassidy, P.; Hitchman, M. A. *Inorg. Chem.* 1977, 16, 1568-1570.

(38) While the $(\text{nmph})_2\text{CuCl}_4$ salt is closest to strict D_{4h} symmetry, its availability only as a pure material precludes the observation of any fine structure in the EPR experiment. Thus delocalization has to be determined for the distorted octahedral salts $\text{K}_2\text{Pd}[\text{Cu}]\text{Cl}_6^{39}$ and $\text{Cd}[\text{Cu}]\text{Cl}_2$,⁴⁰ in which the copper is doped into a host lattice.

(39) Chow, C.; Chang, K.; Willet, R. D. *J. Chem. Phys.* 1973, 59, 2629-40.

(40) Thornley, J. H. M.; Mangum, B. W.; Griffiths, J. H. E.; Owen, J. *Proc. Phys. Soc. London* 1961, 78, 1263.

(41) Cohen, S. L.; Didziulis, S. V.; Solomon, E. I., unpublished results.

(42) McGarvey, B. R. *J. Phys. Chem.* 1967, 71, 51-67.

Table V. Results of g Value Calculations for $C_s(\text{met})$ and C_1 Approximations

	value before adjustment	value after adjustment	original Cu character in ground state wave function	adjusted Cu character in ground state wave function
$C_s(\text{met})$				
g_x	2.046	2.059		
g_y	2.067	2.076	31%	40%
g_z	2.159	2.226		
C_1				
g_x	2.058	2.061		
g_y	2.079	2.091	33%	42%
g_z	2.157	2.226		
experimental values: $g_x = 2.042$; $g_y = 2.059$; $g_z = 2.226$				

the approach shown in eq 4 is applied to this reappportioned region II calculation, then $g_{\parallel} = 2.221$, $g_{\perp} = 2.048$ is obtained with 61% ground-state metal character. Two other calculations giving ground state wave functions are available for D_{4h} CuCl_4^{2-} . An INDO calculation⁴⁶ gave a ground-state delocalization of 49% which leads to $g_{\parallel} = 2.119$, $g_{\perp} = 2.042$. Alternatively, a LCAO-MO-SCF calculation⁴⁷ gave 96% copper character in the ground state and $g_{\parallel} = 2.488$, $g_{\perp} = 2.116$. In both of these latter cases it is apparent that the calculated g values are far off from experiment.

(ii) **Hyperfine Values.** Hyperfine values for copper can also be calculated from the spin-orbit corrected ground state obtained from the $X\alpha$ calculation rather than using the perturbation expressions, eq 6. Over a manifold $|LS\rangle$, Abragam and Pryce⁴⁸ have obtained expressions for the hyperfine operator:

$$A_i = P_d [L_i + (\xi L(L+1) - \chi) S_i - (\frac{3}{2}) \xi L_i (L \cdot S) - (\frac{3}{2}) \xi (L \cdot S) L_i] \quad (8)$$

where $i = x, y, z$, $\xi = \frac{2}{2l+1}$, κ is the Fermi contact term, and P_d is the same as in (6). By treating A_i in a manner analogous to the Zeeman operator considered above and operating only over the metal part of the spin-orbit corrected ground state wave function, one can obtain the elements of the A^2 tensor. Diagonalization yields the square of the principal values of the hyperfine interaction as well as eigenvectors which will transform the starting basis into one in which A^2 is diagonal. The sign of the A values can be obtained by evaluating A_i directly in a basis set in which A^2 is diagonal. Values for κ and P_d can be taken from the literature, or fit to the data.

(iii) **Applications to the Blue Copper Site.** The results of our g value calculation on both the $C_s(\text{met})$ and C_1 sites for plastocyanin are given in Table V. In both cases the change in delocalization required to obtain a fit to the data was small, less than 10%. The final spin-orbit corrected wave functions were for $C_s(\text{met})$

$$\begin{aligned} \psi_0 = & 40\% \text{ Cu} [0.99(x^2 - y^2) - 0.10(xz) - 0.10(yz)] \\ & + 0.8\% \text{ Cu} [0.71(p_x) + 0.71(p_y)] \\ & + 36\% \text{ S}_{\text{cys}} [p_{\pi}] \\ & + 4.8\% \text{ N} [0.99 p_{\sigma}] + 4.8\% \text{ N} [0.9 p_{\sigma}] \\ & + 0.01\% \text{ S}_{\text{met}} \end{aligned} \quad (9a)$$

and for the C_1 site

$$\begin{aligned} \psi_0 = & 42\% \text{ Cu} [0.99(x^2 - y^2) + 0.06(yz) + 0.03(xz) + 0.04(z^2)] \\ & + 0.9\% \text{ Cu} [0.80(p_x) + 0.56(p_y)] \\ & + 0.1\% \text{ Cu} [s] \\ & + 32\% \text{ S} [p_{\pi}] \\ & + 5.4\% \text{ N}_1 [p_{\sigma}] \\ & + 3.9\% \text{ N}_2 [p_{\sigma}] \end{aligned} \quad (9b)$$

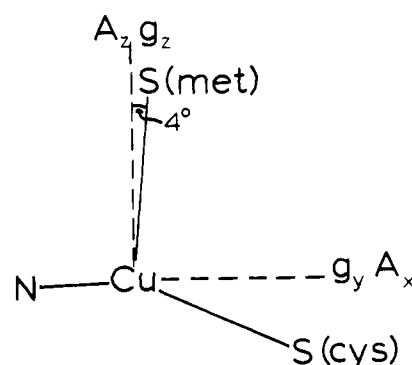
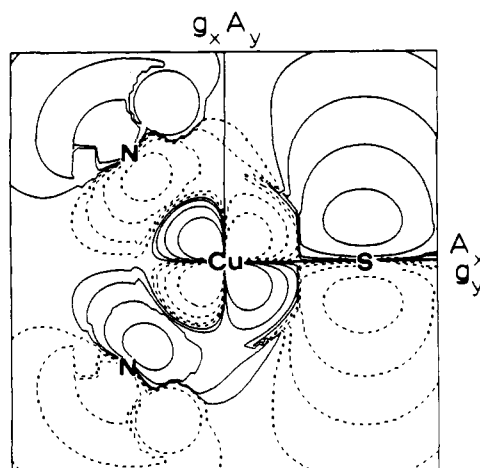
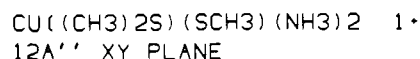


Figure 10. Orientation of the ground state wave function for the $C_s(\text{met})$ approximation to plastocyanin. Top: contour indicating the orientation of the g^2 and A^2 tensors in the plane containing both nitrogens and the copper. Bottom: orientation of the g^2 and A^2 tensors with g_x orthogonal to the plane of the diagram.

A contour diagram showing the orientation of both the g^2 and A^2 tensors for the $C_s(\text{met})$ site is shown in Figure 10. Several features are of note.

First, it is evident that the unpaired electron is strongly delocalized over both the copper (40%) and the sulfur (36%) centers. An examination of the contour diagrams in Figure 10 shows two lobes of the $d_{x^2-y^2}$ orbital directed toward the nitrogen atoms, while the other two lobes are involved in a π -antibonding interaction with a thiolate sulfur p orbital. The large amount of delocalization over the sulfur suggests that it is the antibonding interaction between the sulfur and the copper which controls the orientation of the $d_{x^2-y^2}$ orbital. This is in contrast to the results obtained from a crystal-field calculation,⁷ which suggested the orientation of the metal orbital was controlled by the relatively strong ligand field associated with the two imidazoles. Since the total nitrogen character is only 11% in the $X\alpha$ calculation, the influence of these ligands is small.

In the site of C_s symmetry, the copper p orbitals are only allowed to mix into this half-occupied orbital in combinations which are antisymmetric with respect to reflection across the mirror plane, while copper s orbitals are group theoretically forbidden from mixing into this level. In the site of C_1 symmetry, no atomic orbitals are prohibited from mixing into this level. However, the contributions of copper s and p orbitals to the ground state of the C_1 site ($\text{Cu } p_{x,y} = 0.9\%$, $\text{Cu } s = 0.1\%$) are quite small.

A small rhombic splitting in the g values is also calculated. As a rhombic splitting was also indicated by our crystal-field computations, a higher resolution EPR spectrum than the previously considered X band data was obtained. Figure 11 shows the results of Q-band EPR on a frozen sample of spinach plastocyanin. A rhombic splitting is clearly discernible with $g_x = 2.042$, $g_y = 2.059$,

(46) Van der Lugt, W. *Int. J. Quantum Chem.* **1972**, *4*, 859.

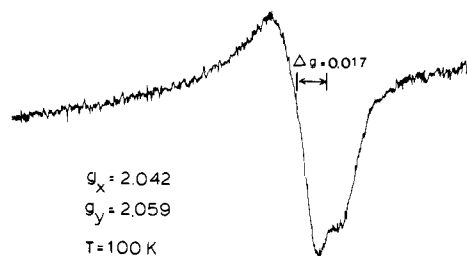
(47) Demuyck, I.; Veillard, A.; Wahlgren, U. *J. Am. Chem. Soc.* **1973**, *95*, 5563.

(48) Abragam, A.; Pryce, M. H. L. *Proc. R. Soc. London A* **1951**, *205*, 135-153.

Table VI. Results of Calculation of Hyperfine Parameters (10^{-4} cm^{-1}) for Plastocyanin and $D_{4h} \text{ CuCl}_4$, Broken Down by Terms in the Hamiltonian

	term in Hamiltonian ^a				total	exptl ^b
	$-P_d\kappa$ ("Fermi contact")	$P_d\xi L(L+1)S_i$ "diagonal spin dipolar"	$-P_d^3/2\xi[L_i(L\cdot S) + (L\cdot S)L_i]$ "off-diagonal orbital dipolar"	P_dL_i		
CuCl_4						
$A_{x,y}$	-121	+72	+15	-34	34.5 ^c	
A_z	-121	-144	+101	-164	164 ^c	
$C_s(\text{met})$ plastocyanin						
A_x	-79	+45	+19	-14	<17 ^d	
A_y	-79	+45	+17	-16	<17 ^d	
A_z	-79	-97	+106	-65	63 ^d	

^aNote that the third term contains both diagonal and off-diagonal elements. The sum of the second term and the diagonal elements of the third term is the dipolar contribution to the hyperfine. ^bAbsolute values are given. ^cFrom ref 39; these are the values for $\text{K}_2\text{Pd}[\text{Cu}]\text{Cl}_4$. ^dFrom ref 1b.

**Figure 11.** Q-band EPR spectrum of the g_{\perp} region of spinach plastocyanin. Field sweep was between 11 275 and 12 275 G while the microwave frequency was 34.282 GHz.

a difference of 0.017. The g value calculation of the C_s site gave $g_y - g_x = 0.017$, in excellent agreement. The origin of this rhombic splitting appears to be related to covalent delocalization over the sulfur p_{π} orbital. If the calculations are repeated setting the sulfur spin-orbit coupling constant to zero, the calculated g value splitting is significantly reduced to 0.002. Since in the coordinate system which diagonalizes g^2 , the sulfur p_{π} orbital character in the ground state, can be denoted as p_x , the only spin-orbit mixing will be with p_y and p_z . In turn, this means that the only contribution to the g values will be to g_y and g_z , not g_x . Thus, the rhombic splitting can be viewed as further evidence for delocalization onto the sulfur p_{π} orbital. Finally, the coordinate system which diagonalized the g^2 tensor is rotated 45° (in the $C_s(\text{met})$ site) relative to the ground-state $d_{x^2-y^2}$ orbital; in the g^2 tensor coordinate system, the orbital can be described as d_{xy} .

The results of calculations of hyperfine parameters for the $C_s(\text{met})$ site with the g value adjusted wave function are presented in Table VI. The agreement with experiment is quite good. In addition, the calculated orientation of A_z in both the C_1 and $C_s(\text{met})$ calculations is within 4° of g_z (Figure 10), consistent with the g and A tensor colinearity experimentally observed. Here, we retained the delocalizations determined from the g value calculations and then fit the hyperfine by varying the value of κ . In performing these hyperfine calculations, we used $P_d = 396 \times 10^{-4} \text{ cm}^{-1}$, which is a weighted average of the free ion P_d values for $^{63}\text{Cu}^{2+}$ ($388 \times 10^{-4} \text{ cm}^{-1}$) and $^{65}\text{Cu}^{2+}$ ($418 \times 10^{-4} \text{ cm}^{-1}$).⁴² A wide range of copper complexes exhibit κ values in the range from 0.22 to 0.32.⁴² For $D_{4h} \text{ CuCl}_4$, the hyperfine values could be fit with $\kappa = 0.300$.

A comparison of the values for the various terms of the hyperfine operator between plastocyanin and $D_{4h} \text{ CuCl}_4^{2-}$ is shown in Table VI. Two factors account for the difference between the "normal" values of $D_{4h} \text{ CuCl}_4^{2-}$ and the "anomalous" small values of plastocyanin. First, the difference in delocalization between the two sites can directly account for about half the difference. This reduces the dipolar term in plastocyanin by about 35% relative

to its value in $D_{4h} \text{ CuCl}_4^{2-}$. The second contribution to the reduction in A_z between the two complexes is in the Fermi contact term. There are two possible effects contributing to the reduction in κ : delocalization and 4s mixing. If the entire reduction is attributed to 4s mixing then on the order of 2.3% 4s character would be required in the ground state.⁴⁹ Alternatively, it has been suggested⁴² that increased covalency can also lower κ values. In $\text{Cu}[\text{S}_2\text{CN}(\text{C}_2\text{H}_5)_2]_2$, a tetragonal copper complex in which substantial Cu s mixing is prohibited by D_{4h} symmetry,^{42,50} a consideration of the Cu hyperfine similar to that in eq 6a and 6b gives delocalization of 50% and κ equal to 0.23. The κ value required to fit plastocyanin is 0.20. In this limit, therefore, about 0.7% s mixing is needed to account for the difference between the calculated and experimental values of the hyperfine splitting in the protein site. SCF-X α -SW calculations predict only 0.1% 4s mixing.

It should be noted that while earlier interpretations^{10a,51} of the small magnitude of A_z involved symmetry-allowed p_z mixing into the metal $d_{x^2-y^2}$ ground state wave function, our calculation indicates that p_z mixing does not occur. Moreover, a consideration of the formulas^{10a} for the effect of p_z mixing on hyperfine values shows that 10% p_z mixing would be required to obtain the experimental A_z in plastocyanin. However, the addition of this much p_z character would move the already negative A_x and A_y to even larger negative values which is not consistent with experiment.

Thus, the high degree of delocalization of the $d_{x^2-y^2}$ orbital of the copper onto the p_{π} orbital of the thiolate in the ground state wave function can largely account for the g values, the orientation of the g^2 tensor, and the small parallel hyperfine coupling constant in plastocyanin. This orientation and delocalization of the ground state may make a significant contribution in defining electron-transfer pathways in the blue copper active site.

Acknowledgment. We thank Keith Johnson for making the X α programs available and for instruction on their use and David Case, Hans U. Güdel, Francisco Leon, and Scott Wallace for useful discussions. In addition, we thank Susan L. Cohen for making available unpublished photoemission results on CuCl_4^{2-} and the National Science Foundation (CHE-82-04841) for support of this research.

Registry No. C_1 , Cs, 96412-07-6; Cs(met), 96412-08-7; Cs(his), 96412-09-8; CH_3S^- , 17302-63-5; $\text{S}(\text{CH}_3)_2$, 75-18-3; Cu, 7440-50-8; CuCl_4 , 15489-36-8; imidazole, 288-32-4; methanethiol, 74-93-1.

(49) The amount of 4s mixing required in the ground state was evaluated by setting the change in hyperfine equal to $1680 \times 10^{-4} \text{ cm}^{-1}$ times the amount of 4s mixing and solving for this amount. The numerical factor $1680 \times 10^{-4} \text{ cm}^{-1}$ is the direct Fermi contact contribution for Cu 4s orbitals.

(50) Reddy, T. R.; Srinivasan, R. *J. Chem. Phys.* 1965, 43, 1404-9.

(51) Sharnoff^{51c} required 12% p_z mixing to fit the g and A values in Cs_2CuCl_4 .